Inclusive Neutron Spectra at 0° from the Reactions Pb(Ne,n)X and NaF(Ne,n)X at 390 and 790 MeV per Nucleon

R. Madey, J. Varga, A. R. Baldwin, B. D. Anderson, R. A. Cecil,[a] G. Fai, P. C. Tandy, and J. W. Watson
Kent State University, Kent, Ohio 44242

and

G. D. Westfall
Michigan State University, East Lansing, Michigan 44823
(Received 18 April 1985; revised manuscript received 22 July 1985)

Inclusive neutron spectra at 0° were measured from both 390- and 790-MeV/u Ne ions on targets of Pb and NaF. A striking peak at a neutron energy slightly below the beam energy per nucleon has a width (in the projectile rest frame) of ~ 58 MeV/c, which is essentially the same for these two energies and these two targets. We suggest that this narrow peak is projectile evaporation and that it is superimposed on the broader fragmentation process predicted by statistical models. The high-momentum region of the cross section may reflect collective behavior.

PACS numbers: 25.70.Np

During the past fifteen years, projectile fragmentation in energetic nuclear collisions has attracted considerable interest both experimentally[1-3] and theoretically.[4-8] These prior studies focused primarily on composite fragments of the projectile. The interpretation of the measurements of these composite fragments requires a careful treatment of Coulomb interactions,[6] Pauli correlations,[7,8] and absorptive distortion.[6] In the present Letter, we focus our attention on the neutrons emitted from the projectile at 0°. The advantage of the neutron measurements is that their interpretation is free from most of the above complications. We will show that 0° neutron spectra suggest that there is a significant contribution from thermalization and subsequent decay, as well as from prompt fragmentation which samples the Fermi momentum distribution of the projectile prior to the collision. The latter subject was addressed previously; for example, in p-nucleus collisions,[9] in relativistic nuclear collisions,[10] and in the context of nuclear structure.[11] We interpret the neutron spectrum in terms of a narrow evaporation peak superimposed on a broader fragmentation peak. This interpretation suggests that the above two reaction mechanisms[12] can be distinguished in neutron spectra at 0°. The ability to distinguish the evaporation process from the reaction mechanism sampling the Fermi-momentum distribution answers an important question raised by Stokstad[12] about the physics of the projectile fragmentation process. The width of the fragmentation peak agrees with that predicted by statistical models of the fragmentation process.[4,5] Also the Fermi momentum extracted from the neutron spectra agrees with values determined from quasielastic electron scattering.[13]

We measured neutron time-of-flight spectra at 0° from collisions of neon ions at two energies (viz., 390 and 790 MeV/u) with an equal-mass (NaF) target and a heavy (Pb) target. The measurements were carried out at the Bevalac accelerator of the Lawrence Berkeley Laboratory.

The apparatus measured the time difference between the detection of a neutron in a mean-timed[14] neutron detector[15] at a distance of 8.0 m from the target and the detection of a neon ion in a beam telescope, which consisted of two NE-102 (76.2×76.2 mm$^2\times0.8$ mm thick) scintillation counters. These two counters were positioned upstream of the target at 54.6 and 79.1 cm. After traversing the beam telescope and the target, the beam was deflected by a "C" magnet (with a 19.7-cm gap) into a reentrant beam dump. The deflection angle was 15° at 390 and 12.5° at 790 MeV/u. The targets were oriented at an angle of 44.3° with respect to the direction of the incident beam. The target thickness traversed by the beam was 4.8 g/cm^2 Pb and 3.0 g/cm^2 NaF. The neutron detector was an NE-102 plastic scintillator, 10.16 cm thick by 25.4 cm high by 101.6 cm wide. Charged particles incident on the neutron detector were vetoed with a 6.4-mm-thick plastic scintillation counter. The flux of charged particles—mainly protons—incident on the detector at 0° was significantly smaller than the neutron flux. Charged particles emitted from the target in a small range of angles about 0° were deflected by the magnet away from the 0° detector. The measured coincidence rate of neutrons in the 0° detector with neutrons in one of the other detectors (e.g., at 15° and 30°) was typically about a few tenths of a percent. Since the efficiency for detection of charged particles is nearly 10 times that for neutrons, the rate of double hits in the 0° detector from a neutron and a charged particle was estimated to be of the order of a few percent. Target-correlated background was determined from measurements with and without a steel shadow shield, 121.4 cm long by 31 cm high by 60 cm wide,

located halfway between the target and the detector. The shadow shield attenuated neutrons by a factor $> 10^3$ at all energies.

The kinetic energy of each detected neutron was obtained from the time of flight measured between an event in the neutron detector and the passage of a beam ion through the mean-timed scintillation counter, located 54.6 cm upstream of the target, in the beam telescope. Absolute cross sections were extracted with detection efficiencies calculated with the code of Cecil, Anderson, and Madey[16] as a function of neutron energy. Tests of these calculations were reported previously.[17] An unambiguous determination of the time of flight required that one, and only one, beam ion be incident on the target during the 400-nsec sampling time; therefore, pileup circuitry rejected an event when two beam pulses occurred within 450 nsec of each other. The intensity of the usable incident beam was about 2×10^5 ions per pulse after a rejection loss of $\sim 60\%$.

The inclusive neutron spectra measured at 0° from Ne ions on NaF and Pb targets are shown in Figs. 1 and 2 for an energy at the center of the target of 390 and 790 MeV/u, respectively. Each of these 0° spectra is characterized by a striking peak at a neutron energy slightly below the beam energy per nucleon. The high-energy exponential tail extends beyond the kinematic limit for nucleon-nucleon collisions even after Fermi motion in the ground states of the target and projectile is taken into account.

Over a narrow interval of neutron momentum in the rest frame of the projectile, the peak of the invariant cross section is represented well by a Gaussian function with a half-width of ~ 58 MeV/c, which is much narrower than that predicted by statistical models of a fragmentation process.[4,5] We suggest that this narrow peak is the result of neutron evaporation from the excited projectile superimposed on a broader fragmentation process. The Lorentz-invariant cross section for the Pb(Ne,n)X reaction at 390 MeV/u is plotted in Fig. 3 versus the momentum of the neutron in the projectile frame. Shown also in Fig. 3 is our decomposition of the invariant cross section σ_I into the sum of three Gaussian functions each centered at a neutron momentum $\bar{P}$ slightly below the beam momentum per nucleon:

$$\sigma_I = \sum_{i=1}^{3} A_i \exp[(P-\bar{P})^2/1.443h_i^2]. \quad (1)$$

Here h_i is the half width at half maximum (HWHM) for the ith component. The Gaussian functions are shown as dashed lines on the low-energy side of the

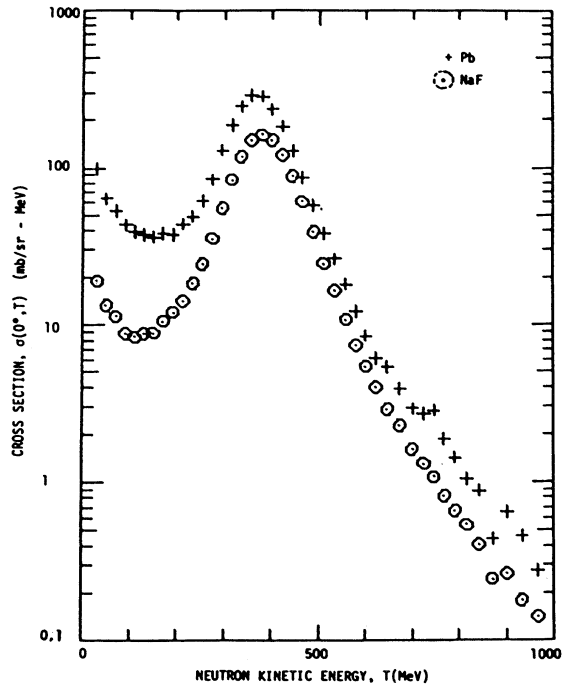

FIG. 1. The double-differential cross section for neutron emission at 0° from collisions of 390-MeV/u Ne ions on NaF and Pb targets vs the neutron kinetic energy in the laboratory.

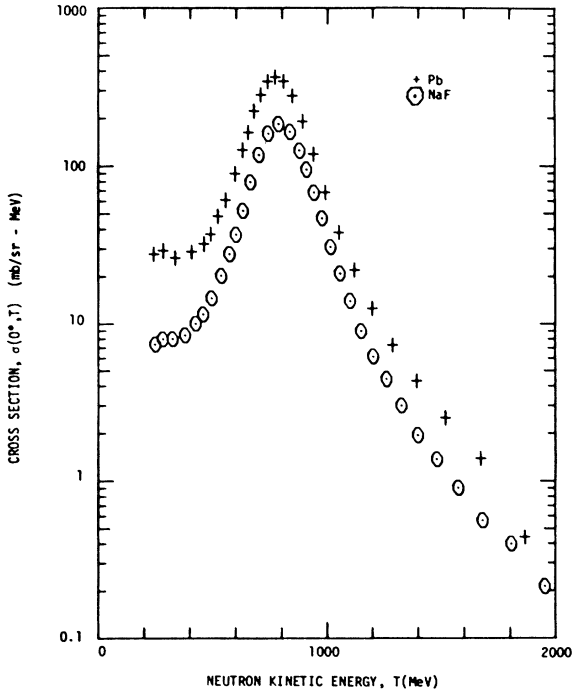

FIG. 2. The double-differential cross section for neutron emission at 0° from collisions of 790-MeV/u Ne ions on NaF and Pb targets vs the neutron kinetic energy in the laboratory.

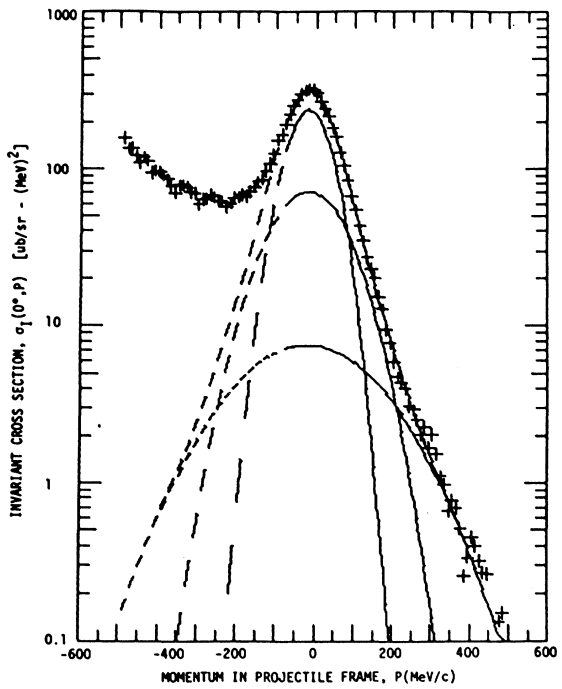

FIG. 3. The Lorentz-invariant cross section for neutron emission at 0° from collisions of 390-MeV/u Ne ions on Pb vs the neutron momentum in the rest frame of the projectile.

peak which contains neutrons from other processes.

The term with the largest amplitude A_1 has a half-width h_1 of ~ 58 MeV/c for a neon projectile at either 390 or 790 MeV/u incident on either the Pb or the NaF target. As discussed above, we interpret this peak as neutron evaporation from the projectile with a temperature of ~ 3.7 MeV.

The second term with amplitude A_2 has a half-width h_2 about 104 MeV/c, which also is essentially identical for the two targets and the two energies. The width of this peak reflects the Fermi momentum P_F of a neutron in the neon projectile. Feshbach and Huang[4] introduced a statistical model to describe the fragmentation of the projectile as a sudden process that releases a neutron with the momentum that it has at the instant of collision. Since the half-width h_2 corresponds to the longitudinal component of the momentum, $h_2^2 = \langle p_z^2 \rangle = \langle p^2 \rangle / 3$. The quantity h_2 contains information on the momentum distribution of neutrons in the projectile. In the Fermi-gas model, $P_F^2 = 5\langle p_z^2 \rangle$. For $h_2 = 104$ MeV/c, we extract $P_F = 233$ MeV/c. These values agree with those given by Goldhaber.[5] Also this determination of P_F agrees with that obtained from quasielastic electron scattering; Moniz *et al.*[13] found $P_F = 235$ MeV/c for ^{24}Mg and $P_F = 221$ MeV/c for ^{12}C with a fitting uncertainty of ± 5 MeV/c. Starting with the same postulates as those of Feshbach and Huang,[4] Goldhaber[5] showed that the momentum distribution of a neutron is not sensitive to the speed of the fragmentation process.

A superposition of only two Gaussian functions, as described above, is insufficient to represent the cross section in the high-momentum region ($\gtrsim 300$ MeV/c in Fig. 3). It is interesting to note that free two-body collisions of nucleons with the Fermi energies appropriate to the target and projectile cannot account for the neutrons that contribute to the high-momentum region of the cross section.

For 1.05-GeV/u C+C collisions, Geaga *et al.*[3] plot the results of their proton-inclusive measurements at 180° in the laboratory together with the results from Papp[18] of the proton-inclusive measurements at 2.5° in the projectile frame. They represent these combined measurements of proton-inclusive distributions by two overlapping Gaussian functions corresponding to our second and third Gaussian functions. Geaga *et al.* parametrize these two Gaussian functions in their Fig. 2. From these parameters, we extract a Fermi momentum of 197 MeV/c for a carbon projectile, which is somewhat smaller than the value obtained from electron scattering. Geaga *et al.* find that the width of the high-momentum component for protons from 1050-MeV/u C or Ar ions on a carbon target is 224 MeV/c (HWHM) with a typical uncertainty of ± 6 MeV/c. For neutrons from a neon projectile on NaF or Pb targets, we extract the same value (within the uncertainties) at 790 MeV/u but a smaller value at 390 MeV/u. These results indicate that the distributions of high-momentum nucleons in the projectile frame are independent of the energy of the incident heavy ion for energies as low as 790 MeV/u, but that limiting fragmentation is not reached at a projectile energy as low as 390 MeV/u.

Here we want to indicate three possible origins for the high-energy tail of the neutron cross section. One possible explanation is that these high-energy neutrons reflect collective behavior from central collisions; for example, with the fireball model,[19] it is possible to fit a smooth background to the $|p| \gtrsim 250$ MeV/c regions of Fig. 3. Another possible explanation involves the high-energy tail of the Fermi distribution of nucleons in the projectile.[9] The fraction of neutrons above the Fermi energy may be large enough to explain the magnitude of the 0° cross section in the high-energy tail. With the values $E_F = 37$ MeV for the Fermi energy and $\rho_0 = 0.17$ fm^{-3} for the bulk nuclear density, we estimate that $\sim 14\%$ of the neutrons in the projectile have energies $E > E_F$. Still another possible mechanism involves the collective backscattering of a neutron in the target from a cluster of nucleons in the projectile. The mean size of the nucleon cluster required to fit the data is ~ 1.8 nucleons.

We are aware of the uncertainty of the decomposition in Eq. (1). We believe that the first two terms are seen clearly in the data. The third term constitutes only a few percent of the integral cross section for neutron momenta above the peak, whereas the second Gaussian curve contains about one third of this integral cross section. The magnitude of the cross section represented by the third Gaussian function is consistent with the findings of Sandoval *et al.*[20] that central collisions represent about 6% of the reaction cross section. While several interpretations of the third (high-momentum) component are possible, we want to emphasize that a manifestation of collective behavior is an especially interesting possibility that may involve nuclear structure effects in relativistic nuclear collisions.

This work was supported in part by the National Science Foundation and the U.S. Department of Energy.

---

[a]Present address: Picker X-Ray, Cleveland, O. 44143.

[1]H. H. Heckman, D. E. Greiner, P. J. Lindstrom, and F. S. Bieser, Phys. Rev. Lett. **28**, 926 (1972).

[2]D. E. Greiner, P. J. Lindstrom, H. H. Heckman, B. Cork, and F. S. Bieser, Phys. Rev. Lett. **35**, 152 (1975); D. L. Olsen, B. L. Berman, D. E. Greiner, H. H. Heckman, P. J. Lindstrom, and H. J. Crawford, Phys. Rev. C **28**, 1602 (1983).

[3]J. V. Geaga, S. A. Chessin, J. Y. Grossiord, J. W. Harris, D. L. Hendrie, L. S. Schroeder, R. N. Treuhaft, and K. Van Bibber, Phys. Rev. Lett. **45**, 1993 (1980).

[4]H. Feshbach and K. Huang, Phys. Lett. **47B**, 300 (1973).

[5]A. S. Goldhaber, Phys. Lett. **53B**, 306 (1974).

[6]W. A. Friedman, Phys. Rev. C **27**, 569 (1983).

[7]G. Bertsch, Phys. Rev. Lett. **46**, 472 (1981).

[8]M. J. Murphy, Phys. Lett. **135B**, 25 (1984).

[9]S. Frankel, W. Frati, O. Van Dyck, R. Werbeck, and V. Highland, Phys. Rev. Lett. **36**, 642 (1976); S. Frankel, Phys. Rev. Lett. **38**, 1338 (1977).

[10]J. Hufner and M. C. Nemes, Phys. Rev. C **23**, 2538 (1981).

[11]J. G. Zabolitzky and W. Ey, Phys. Lett. **76B**, 527 (1978).

[12]R. G. Stokstad, Comments Nucl. Part. Phys. **13**, 231 (1984).

[13]E. J. Moniz, I. Sick, R. R. Whitney, J. R. Ficenec, R. D. Kephart, and W. P. Trower, Phys. Rev. Lett. **26**, 445 (1971).

[14]A. R. Baldwin and R. Madey, Nucl. Instrum. Methods **171**, 149 (1980).

[15]R. Madey, J. W. Watson, M. Ahmad, B. D. Anderson, A. R. Baldwin, A. L. Casson, W. Casson, R. A. Cecil, A. Fazely, J. M. Knudson, C. Lebo, W. Pairsuwan, P. J. Pella, J. C. Varga, and T. R. Witten, Nucl. Instrum. Methods **214**, 401–413 (1983).

[16]R. A. Cecil, B. D. Anderson, and R. Madey, Nucl. Instrum. Methods **161**, 439 (1979).

[17]J. W. Watson, B. D. Anderson, A. R. Baldwin, C. Lebo, B. Flanders, W. Pairsuwan, R. Madey, and C. C. Foster, Nucl. Instrum. Methods **215**, 413 (1983).

[18]J. Papp, Ph.D. thesis, University of California, Berkeley, Report No. LBL-3633, 1975 (unpublished).

[19]G. D. Westfall, J. Gosset, P. J. Johansen, A. M. Poskanzer, W. G. Meyer, H. H. Gutbrod, A. Sandoval, and R. Stock, Phys. Rev. Lett. **37**, 1202 (1976); J. Gosset, H. H. Gutbrod, W. G. Meyer, A. M. Poskanzer, A. Sandoval, R. Stock, and G. D. Westfall, Phys. Rev. C **16**, 629 (1977).

[20]A. Sandoval, R. Stock, H. E. Stelzer, R. E. Renfordt, J. W. Harris, J. P. Brannigan, J. B. Geaga, L. J. Rosenberg, L. S. Schroeder, and K. L. Wolf, Phys. Rev. Lett. **45**, 874 (1980).